Available online at www.sciencedirect.com
SCIENCE DIRECT®
Journal of Power Sources 114 (2003) 213–227
JOURNAL OF POWER SOURCES
www.elsevier.com/locate/jpowsour

# Modelling for part-load operation of solid oxide fuel cell–gas turbine hybrid power plant

S.H. Chan*, H.K. Ho, Y. Tian

*Fuel Cells Strategic Research Programme, School of Mechanical and Production Engineering, Nanyang Technological University, 50 Nanyang Avenue, Singapore 639798, Singapore*

Received 8 August 2002; accepted 31 October 2002

**Abstract**

This paper presents the work on part-load operation of a power generation system composed of a solid oxide fuel cell and a gas turbine (SOFC–GT) which operate on natural gas. The system consists of an internal reforming SOFC (IRSOFC) stack, an external combustor, two turbines, two compressors, two recuperators and one heat-recovery steam generator (HRSG). Based on experience in different levels of modelling of the fuel cell, fuel cell stack and integrated system and the inherent characteristics of a IRSOFC–GT hybrid power plant, a practical approach for simplifying part-load operation of the system is proposed. Simulation results show that an IRSOFC–GT hybrid system could achieve a net electrical efficiency and system efficiency (including waste heat recovery for steam generation) of greater than 60 and 80%, respectively, under full-load operation. Due to the complexity of the interaction of the components and safety requirements, the part-load performance of a IRSOFC–GT hybrid power plant is poorer than that under full-load operation.


*Keywords:* Hybrid power system; SOFC stack modelling; Part-load operation

## 1. Introduction

A solid oxide fuel cell and gas turbine (SOFC–GT) hybrid system has been considered as competitive in the market of distributed/residential power supply and mobile applications [1–3]. As a stand-alone power station, its power output should be able to adjust quickly to follow the load demand. Thus, part-load performance and operational stability/safety are key issues for commercialisation. Campanari [4] calculated separately (i) the performance of a turbine at different turbine inlet temperatures (TIT), shaft speeds and pressure ratios and (ii) the lower heating value (LHV) efficiency of a SOFC stack at different air/fuel flow rates (decrease of air flow and air utilisation simultaneously). The data were then combined to determine the overall performance of the hybrid power plant. When load decreases, the turbine and the fuel cell stack both reduce their respective power output to follow the demand. The weaknesses of this approach include: (i) speed matching between the turbine and the air compressor was ignored; (ii) the turbine mass flow rate, which links the two sub-systems, was not directly involved in the performance map of the turbine (pressure ratio and speed were used instead) and the fuel cell stack (air utilisation and current density were used instead). The author assumed that the speed and inlet temperature of the gas turbine could be adjusted to achieve the maximum power output at different mass flow rates and is sufficiently powerful to drive the air compressor and generator. The details of both the component matching of the gas turbine–compressor machine and the TIT control method were not mentioned. Costamagna et al. [5] also conducted a part-load performance study on a SOFC–GT hybrid system. A similar configuration of system was proposed and the efficiency of the plant was studied under constant and variable speed conditions on the assumption that a variable speed control system was available for the turbine. The authors concluded that the use of a turbine with a variable speed control is of paramount importance if the plant is to operate at high efficiency. There was no discussion, however, on component matching in terms of thermal and mechanical aspects.

In this paper, an approach is proposed for part-load operation of a SOFC–GT hybrid system in which the fuel cell has an internal reformer, a so-called IRSOFC–GT system. Component matching, including energy and rotational speed match, of the turbine and air compressor is considered. In addition, the usual practice of keeping the

* Corresponding author. Tel.: +65-790-4882; fax: +65-792-4062.
*E-mail address:* mshchan@ntu.edu.sg (S.H. Chan).

0378-7753/02/$ – see front matter 
PII: S0378-7753(02)00613-4

**Nomenclature**

| | |
|---|---|
| $C_p$ | specific heat at constant pressure (J kg$^{-1}$ K$^{-1}$). |
| $h$ | enthalpy (kJ kg$^{-1}$) |
| $k$ | air compression factor |
| $\dot{m}$ | mass flow rate (kg s$^{-1}$) |
| $[\dot{m}]$ | corrected mass flow |
| $N$ | rotational speed (rpm) |
| $\dot{n}$ | molar flow rate (kmol h$^{-1}$) |
| $[N]$ | corrected rotational speed |
| $p$ | pressure (bar) |
| $Q$ | heat transfer (kJ) |
| $T$ | temperature (K) |

*Greek letters*

| | |
|---|---|
| $\eta$ | efficiency |
| $\theta$ | temperature ratio |

*Subscripts*

| | |
|---|---|
| C | compressor |
| g | gas |
| GT | gas generator turbine |
| PT | power turbine |
| s | steam |
| std | standard |
| w | water |

turbine operating at constant speed is adopted. The ultimate aims are to achieve simple and safe operation of SOFC–GT hybrid system under part-load conditions, which are the key issues for commercialisation.

## 2. System configuration

A typical IRSOFC–GT hybrid system is examined in this study and is shown schematically in Fig. 1. The system consists of one SOFC stack, one combustor, one single-spool gas turbine (GT), one free-rotating power turbine (PT), two compressors, two recuperators, and one heat-recovery steam generator (HRSG). An inverter with a typical efficiency of 96.5% is assumed. The mechanical work produced by the GT is used to drive the air compressor, and the sole mechanical power available for electrical power generation is from the PT. The bypass of the turbine (upper dashed line) is for emergency gas exit. The dashed lines from the fuel and the air compressors represent the fuel and air lines, respectively, are activated for start-up and part-load operations. Since the fuel flow rate is low (about 0.044 kg s$^{-1}$ of natural gas for a 1.3 MW power plant), the efficiency of the fuel compressor, which is powered by electricity from batteries/electricity grid when the plant starts up, can be assumed to be constant. After the plant starts, the fuel compressor will use the electricity generated from the power plant itself. This power consumption should be deducted from the total electrical power generated by the system in the overall efficiency calculation.

The compressed fuel and air are preheated in their respective recuperators prior to entering the IRSOFC stack. Natural gas and air are channelled through the anode and cathode compartments, respectively. Natural gas is internally reformed in the anode compartment and hydrogen-rich products are produced. The electrochemical reaction occurs at the three-phase boundaries (TPB) of the electrodes and produce ionic current through the electrolyte and electronic

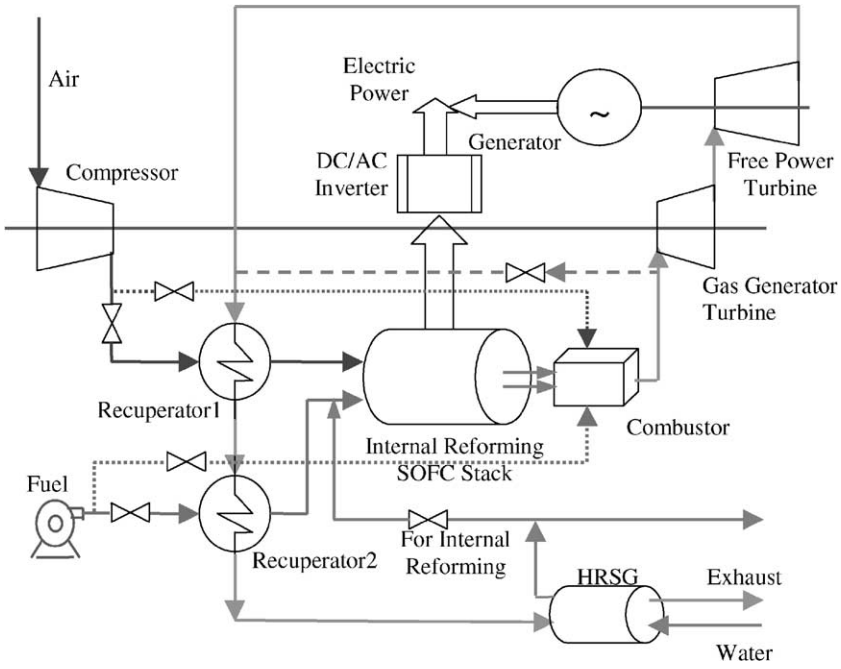


Fig. 1. Configuration of SOFC–GT hybrid power system.

current across the electrodes. Electrical energy is produced together with heat generation during the process. The heat generated is partly dissipated to the surroundings, partly used to reform the natural gas, and partly used to heat up the feedstock gases. The high-temperature effluent gases from the IRSOFC stack, which consist of unutilised reformed natural gas and depleted air, are channelled to a combustor where residual fuels (hydrogen, methane and carbon monoxide) react with the depleted air from the cathode compartment. The amount of residual fuels in the exit of IRSOFC stack can be determined from the operating conditions of the IRSOFC. Because the operating temperature of the IRSOFC is around 1000 °C, excess air is required to ensure that the combustor, and hence its exit gas temperature, does not exceed the allowable turbine inlet temperature (TIT, about 1400 K). In this model, part of the air from the air compressor can be directed to the combustor to 'dilute' the combustion temperature. Under normal operation, no fuel is directly channelled to the combustor.

The combusted gas mixture flows through the GT and mechanical power is produced. This power is consumed by the compressor to compress the air to its required pressure. Subsequent expansion through the PT produces additional mechanical power which is used to generate the electricity. The effluent gases from the PT pass through a series of two recuperators where preheating of air and fuel occurs. The function of the HRSG is to generate steam for internal reforming and industrial/residential use.

Previous studies have shown that the hybrid system can reach a very high electrical efficiency when operating at full load [6,7]. Difficulties arise under part-load operation, however, the complex interaction of system components. During load variations, the shaft speed, pressure ratio and efficiency of the compressor and turbine follow the change of mass flow rate and gas temperature, but the shaft speed and power of both turbomachines are the same as they are rigidly coupled to each other. The following two problems are the most critical.

(i) In a system where the SOFC stack, which operates between 850 and 1000 °C, is treated as the 'combustor' of the gas turbine, the TIT of GT should follow the change in temperature of the SOFC stack. When the mass flow rate through the stack is reduced during part-load operation, the GT may not be able to maintain its required power output.
(ii) The air compressor and the GT have the same shaft speed as they are connected to each other by a rigid shaft, while the power of the GT is equal to the power demand of the air compressor divided by the mechanical efficiency. It can be assumed that there is a variable speed control system available, but because the GT is sensitive to the change of mass flow rate and temperature of the exhaust gas, the GT may not be able to provide sufficient power to drive the compressor and achieve the required pressure ratio across the compressor. This causes deterioration in the performance of the integrated system. In addition, the complexity of adjusting the speed of GT and compressor and the delay response will result in poor safety and poor load-following capability.

In this study, a new approach is proposed for system part-load operational control. In this approach, an external combustor plays a critical role. The start-up and part-load operation of the system are described below.

(i) When the system starts, fuel is directly channelled to the external combustor. Part of the air from an air compressor is preheated in recuperator 1 before flowing through the SOFC stack to heat up the stack; the rest of the air is channelled to the combustor directly for combustion. The turbine speed increases gradually to its designed speed. When the stack temperature reaches 700 °C or higher, the fuel flow is gradually channelled to the SOFC stack and the heat generated from the electrochemical reaction increases the stack temperature until an equilibrium with the nominal operating temperature is reached. The rate of temperature rise can be adjusted by controlling the rate of air flow to the stack. When no fuel is directly combusted in the combustor, the system will operate at its full-load condition.
(ii) If a small load excursion occurs, the fuel and air flow rates through the SOFC stack should be reduced, and hence the mass flow in the GT is also reduced. In this case, additional fuel is combusted in the combustor to improve the gas temperature prior to entering the GT in order to achieve the designed operating point of the GT. No additional cooling air is required in this case.
(iii) If a medium or large load excursion occurs and causes significant decrease in the mass flow rate of the gas, the increase of gas temperature alone by burning additional fuel is not sufficient for the GT to produce power to drive the compressor. In addition, the TIT may have reached its temperature limit and thus diluting air is necessary to maintain normal operation of the GT.
(iv) If the load excursion persists for a long time, the GT may have to reduce its power output by decreasing the flow rate of fuel to the combustor. This results in a low pressure ratio across the air compressor and shaft speed. The reduced pressure ratio decreases the voltage output and the efficiency of the stack. The decrease in fuel demand of the combustor will, however, reduce the effect of this operation on the overall system efficiency. Since this operation involves the control of shaft speed in addition to the control of the fuel and the air flow rates, it is quite a complex process and thus suitable only for use in a long period of part-load operation.

In this configuration, the external combustor serves the purpose of separating the operation of the SOFC stack from that of gas turbine system, so that they are not thermally dependent on each other. Moreover, it takes advantage of the inherent characteristics of the SOFC–GT hybrid system, and the reduced load in part-load operation control affects mainly the power output of the SOFC stack.

## 3. Modelling

### 3.1. Fuel cell and internal reforming fuel cell stack

The fuel cell model developed in this study is based on the design of Siemens Westinghouse. The geometric and performance data of the SOFC can be obtained from [8,9].

The SOFC and SOFC stack models consist of both electrochemical and thermal models; which are integrated into the respective sub-systems. The key parameter in the computation is the operating temperature which is dependent on various operating and design data. Details of the modelling of the fuel cell, internal reforming and fuel cell stack can be found in our previous studies [6,7].

### 3.2. Compressor and gas turbine models

The simplified compressor–IRSOFC–combustor–GT–PT system is shown schematically in Fig. 2. Typical turbine maps are used in the modelling. The compressor map is based on a DLR centrifugal compressor map, while the turbine map is for a NASA-CR-174646 axial turbine. The original and smoothened data files of these turbomachines were obtained from the manufacturers. The original data files consist of the measured values which are not evenly distributed over the range of interest and they are not arranged in any specific order. The measured data are post-processed and the output data are stored for later use. The refined data are arranged in ascending order of regular speed increments. For each speed line, the pressure ratio and efficiency that correspond to each possible mass flow rate are listed. There is same number of data points for each speed line.

To determine the operating points of the compressor and turbine from the maps, the mass flow rate together with either the speed or pressure has to be given. Difficulties may arise, however, in data searching because each speed line contains a wide range of mass flow rate and pressure ratio values, and overlapping of mass flow rate occurs between different speed lines. Thus, to determine a unique operating status, the relationship between mass flow rate and pressure ratio must be established. To resolve this problem, β lines are used as an auxiliary coordinate to determine an operating status. These are lines of pressure ratio over mass flow rate that result in unique intersections with the speed line. The data search routine will produce 20 β lines that are equally spaced parabolas in the plane of {mass flow rate, pressure}.

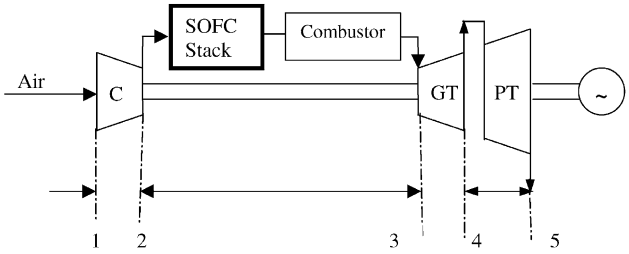


Fig. 2. Once-through gas-cooled steam generator.

All β lines are described by a second order polynomial in the simulation program.

To make this model capable of simulating various sizes of power plant, a standard operating requirement is set and corresponds to a specific corrected mass flow rate, $\dot{m}_{\mathrm{std}}\sqrt{T_{1,\mathrm{std}}}/p_{1,\mathrm{std}}$, and a corrected speed, $N_{\mathrm{std}}/\sqrt{T_{1,\mathrm{std}}}$, at full load. When the system operates at part-load conditions, its corrected mass flow rate and corrected speed are divided by their respective standard values, i.e.

$$m_{\mathrm{r}} = \frac{\dot{m}}{\dot{m}_{\mathrm{std}}}\frac{\sqrt{T_1 T_{1,\mathrm{std}}}}{p_1/p_{1,\mathrm{std}}}, \qquad n_{\mathrm{r}} = \frac{N/N_{1,\mathrm{std}}}{\sqrt{T_1 T_{1,\mathrm{std}}}} \tag{1}$$

The benefit of doing this is obvious, namely: (i) the actual compressor and turbine mass flow rates are hidden from the system operation, thus switching to other types of compressor and turbine is easy; (ii) the nominal power rating of the plant can be changed desirably. When simulating a larger or smaller power plant, only the above standard values have to be changed.

### 3.3. Combustor model

All residual fuels from the stack are burned away in the combustor, which increases the temperature of the exhaust gas. The following reactions are considered in calculating the exit gas temperature of the combustor

$$\mathrm{CH_4} + 2\mathrm{O_2} = \mathrm{CO_2} + 2\mathrm{H_2O} + Q_{\mathrm{CH_4}} \tag{2}$$

$$\mathrm{CO} + \tfrac{1}{2}\mathrm{O_2} = \mathrm{CO_2} + Q_{\mathrm{CO}} \tag{3}$$

$$\mathrm{H_2} + \tfrac{1}{2}\mathrm{O_2} = \mathrm{H_2O} + Q_{\mathrm{H_2}} \tag{4}$$

Assuming that the process is adiabatic, the enthalpy of the reactants with combustion efficiency taken into account will be equal to the enthalpy of the products. Knowing the temperature of the reactants, the product temperature can be calculated by iteration as the properties of each product gas are temperature-dependent. The combustion efficiency is set conservatively at 98%, though it can be as high as 99.5% [4].

### 3.4. Heat-recovery steam generator (HRSG) model

The distribution of temperature along the axis of a HRSG, which is a counter flow heat exchanger, is shown in Fig. 3.

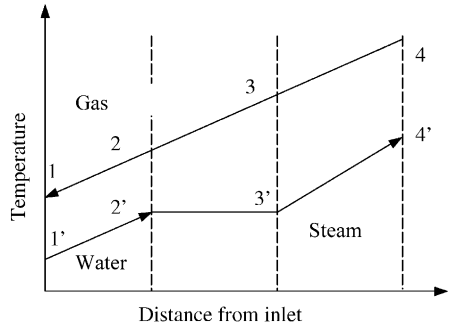


Fig. 3. Compressor–fuel cell–combustor–gas turbine–power turbine engine.

The heated fluid can be divided into three sections, viz. preheating (sub-cooled), boiling (saturated), and overheating (superheat). At each heat-transfer section, the following establish the heat balance

$$\dot{m}_g c_{pg}(T_2 - T_1) = \dot{m}_w c_{pw}(T_2' - T_1') = \Delta H_1 \quad (5)$$

$$\dot{m}_g c_{pg}(T_3 - T_2) = \dot{m}_w h_{fg} = \Delta H_2 \quad (6)$$

$$\dot{m}_g c_{pg}(T_4 - T_3) = \dot{m}_s c_{ps}(T_4' - T_3') = \Delta H_3 \quad (7)$$

where $\dot{m}_g$ is the mass flow rate of the gas; $\dot{m}_w$ the flow rate of water; $c_{pg}$, $c_{pw}$ are specific heats at constant pressure for gas and water, respectively; $h_{fg}$ is the latent heat of water.

Assuming that the exit temperatures of the gas $T_1$ and steam $T_4'$ are known, the unknown variables are the water flow rate $\dot{m}_w$, and the gas temperatures $T_2$ and $T_3$. Combining these equations, the temperature changes and heat transfer of each section can be determined. Once the heat transfer of each section is known, the heat-transfer area of each section can be sized. If $U$ is the overall heat-transfer coefficient and $A$ is the heat-exchange area, the heat transfer in each section can be determined by

$$\Delta H_i = U_i A_i \Delta T_{mi}, \quad i = 1, 2, 3 \quad (8)$$

where $\Delta T_m$ is the log mean temperature difference defined as

$$\Delta T_m = \frac{1}{L}\int_0^L \Delta T; \qquad dx = \frac{\Delta T_0}{L}\int_0^L \left(\frac{\Delta T_L}{\Delta T_0}\right)^{x/L};$$
$$dx = \frac{\Delta T_0 - \Delta T_L}{\ln(\Delta T_0)/(\Delta T_L)} \quad (9)$$

If $U_i$ of each section is known, then the total area of HRSG can be obtained, i.e.

$$A = A_1 + A_2 + A_3 \quad (10)$$

The typical overall heat-transfer coefficient for preheating, boiling and mist-flow is 1360 W (m$^2$ °C)$^{-1}$ (240 Btu (h ft$^2$ °F)$^{-1}$), 1474 W (m$^2$ °C)$^{-1}$ (260 Btu (h ft$^2$ °F)$^{-1}$) and 1190 W (m$^2$ °C)$^{-1}$ (210 Btu (h ft$^2$ °F)$^{-1}$), respectively [10].

Under designed operating conditions, the actual performance of HRSG can be determined by combining Eqs. (5)–(9). The unknown variables are $h_1$, $h_2$, $h_3$, $A_1'$, $A_2'$, $A_3'$ (the 'actual' area of each section has changed under different flow conditions) and $\dot{m}_w$ or $h_4'$, depending on the different assumptions made. In other words, this depends on whether the output steam temperature is fixed and the water flow rate is adjusted automatically during part-load operation, or the water flow rate is directly given. Thus, there are seven unknown variables and six equations available. Eq. (7) can be obtained from

$$A_1' + A_2' + A_3' = A \quad (11)$$

Solving these combined equations simultaneously, the HRSG performance under system part-load conditions can be determined.

### 3.5. Component matching

For the system shown in Fig. 2, the component matching of the compressor–fuel cell–combustor–GT–PT system includes mass flow, energy and rotational speed matching. At a steady-state condition, the air compressor and the GT are running at the same shaft speed as they are directly coupled. Defining corrected speeds for both GT and air compressor as $N_{GT}$ and $N_C$, respectively, then,

$$[N_{GT}] = \frac{N_{shaft}}{\sqrt{T_{03}}} = \frac{N_{shaft}}{\sqrt{T_{01}}}\sqrt{\frac{T_{01}}{T_{03}}} = [N_C]\sqrt{\frac{T_{01}}{T_{03}}} \quad (12)$$

And the corrected mass flow rates are, respectively

$$[\dot{m}_{GT}] = \frac{\dot{m}_3\sqrt{T_{03}}}{p_{03}} = \frac{\dot{m}_1\sqrt{T_{01}}}{p_{01}}\frac{p_{01}}{p_{02}}\frac{p_{02}}{p_{03}}\sqrt{\frac{T_{03}}{T_{01}}}\frac{\dot{m}_3}{\dot{m}_1}$$
$$= [\dot{m}_C]\frac{p_{01}}{p_{03}}\frac{p_{02}}{p_{03}}\sqrt{\frac{T_{03}}{T_{01}}}\frac{\dot{m}_3}{\dot{m}_1} \quad (13)$$

The inlet pressure and temperature of the GT are determined from the conditions of the SOFC stack and the combustor, while the pressure ratio across the GT can be determined from the power balance between the two turbomachines.

The changes of enthalpy across the compressor and GT are

$$\frac{\Delta h_C}{\theta_{01}} = \frac{c_{pC}T_{std}}{\eta_C}\left[\left(\frac{p_{02}}{p_{01}}\right)^{(k-1)/k} - 1\right] \quad (14)$$

$$\frac{\Delta h_{GT}}{\theta_{03}} = c_{PT}T_{std}\eta_T\left[1 - \left(\frac{p_{03}}{p_{04}}\right)^{(k-1)/k}\right] \quad (15)$$

and the power balance yields

$$\Delta h_C = \eta_m \Delta h_{GT} \quad (16)$$

where $\theta_{01} = T_{01}/T_{std}$; $\theta_{03} = T_{03}/T_{std}$; $\eta_m$ is the mechanical efficiency.

The flowcharts for system component matching and part-load operational control are shown in Fig. 4a and b, respectively.

### 3.6. System model

In SOFC–GT hybrid system simulation, there are two important iteration loops. One is to calculate the stack temperature in the SOFC stack model, which is unknown at the beginning of the computation but is necessary for both reforming and electrochemical reaction calculation. The other is to determine the corrected speed and additional fuel/air flow rate for the compressor–SOFC stack–GT system, which requires heat, flow, and shaft speed matching under both full-load and part-load operations. Since both the compressor and GT performance calculation requires a corrected mass flow rate, tedious iteration is unavoidable.

For the whole system model, since the recuperators need the heating fluid parameters (such as the exit gas temperature of the turbine), which are not known at the beginning of the simulation, a set of initial parameters has to be assumed in order to run the system model until convergence is met eventually.

The flowchart for system simulation is presented in Fig. 5. The details of IRSOFC stack simulation can be obtained from our previous studies [6,7].

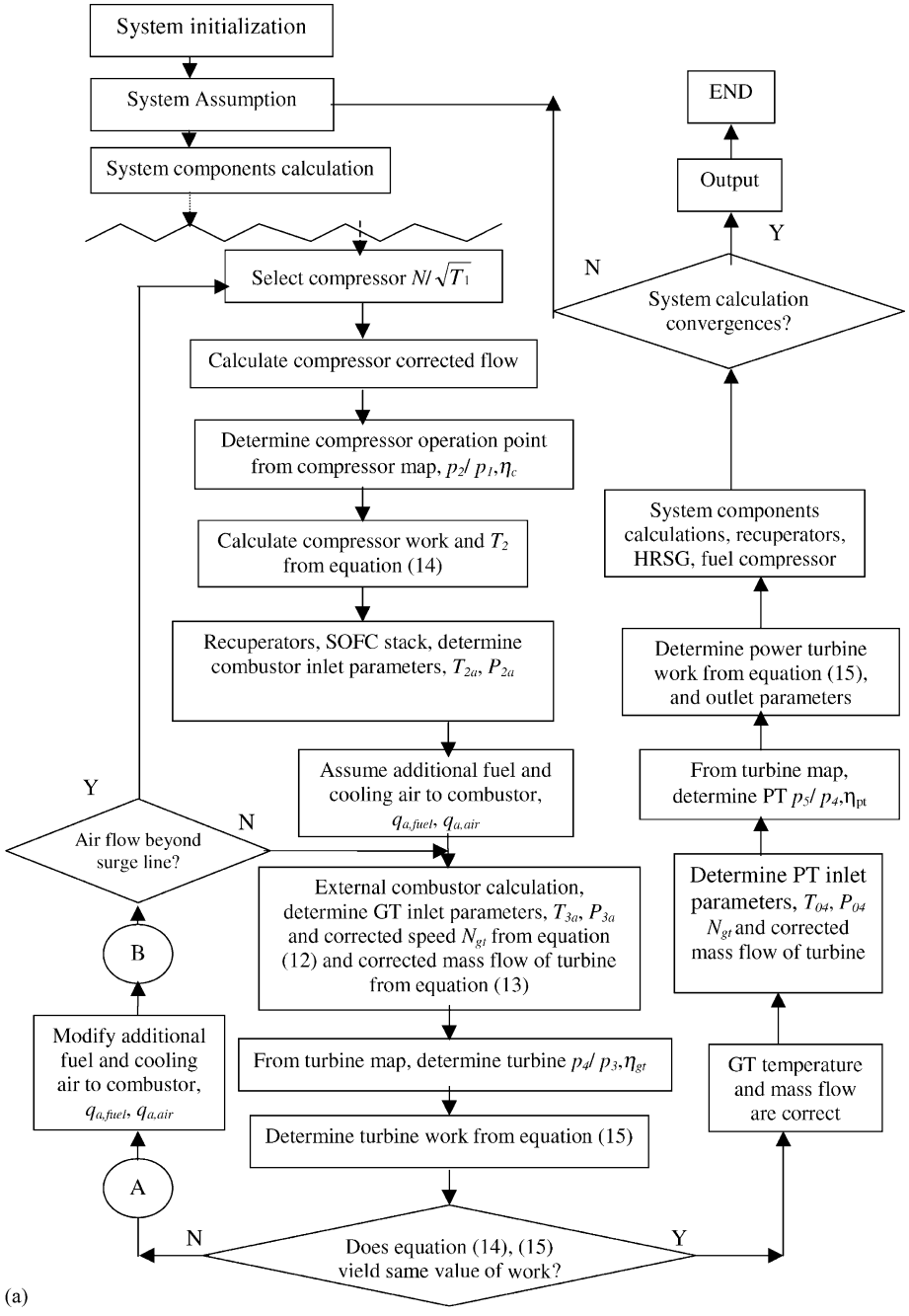


Fig. 4. (a) Algorithm for compressor–SOFC–combustor–GT component matching; (b) algorithm for system fuel/cooling air control under part-load operations.

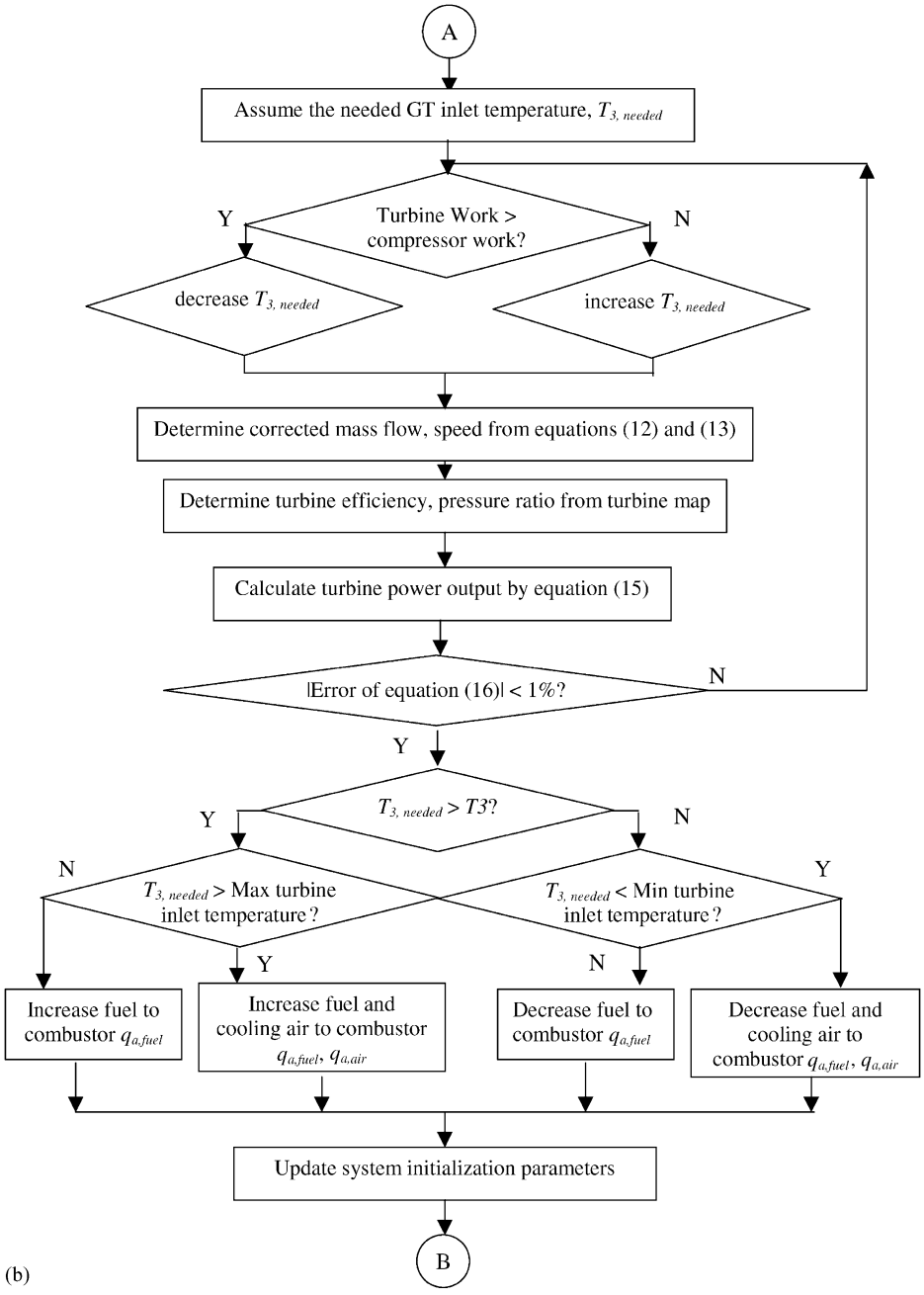


Fig. 4. (*Continued*).

## 4. Simulation results

The maps for the compressor, GT and PT used in this model are shown in Figs. 6–8, respectively. Note that, the dotted lines refer to the β lines, as mentioned earlier. In the proposed system, part of the steam is used for internal reforming and the remainder can be used for residential or industrial applications. The inlet water and outlet steam of the HRSG are set to 98 and 110 °C, respectively. The mass flow rate of water is assumed to be automatically adjusted by a flow controller during system load variation. Under part-load operations, the mass flow rate and inlet temperature of the heating fluids in the HRSG vary with the change of load. In this model, the heat-exchange surface is assumed to be 3 $m^3$, and the effect of temperature on the specific heat of fluids is considered. The effect of mass flow rate of heating fluids on the steam yield is shown in Figs. 9 and 10. The results show that, with the control settings made above and assuming that the gas inlet temperature is fixed at 850 °C, the mass flow rate of steam increases with increase in the mass flow rate of heating gas. This, in turn, causes an increase in the exit temperature of the gas. The effect of the inlet temperature of heating fluids on the steam yield is shown in Figs. 11 and 12. Similar to the data given in Figs. 9 and 10,

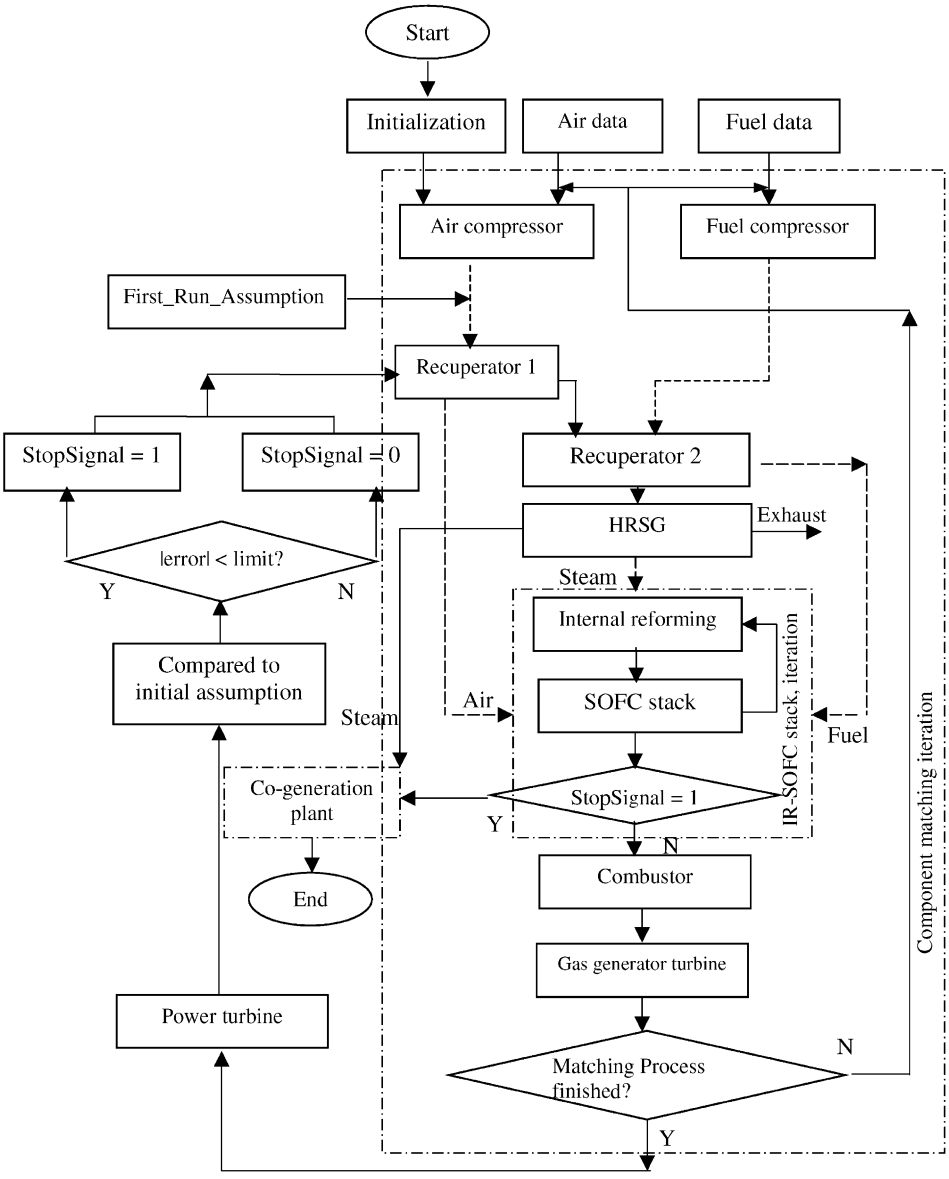


Fig. 5. Flowchart of system program.

the mass flow rate of steam and the exit temperature of gas, both increase with increase in the inlet temperature of the heating fluids.

It should be noted that the system components were designed for full-load operation in a 1.7 MW plant. The major operating parameters of the fuel cell stack are listed in Table 1, and the system performance is summarised in Table 2. Results show that when the cells operate at 0.619 V, the power density is 155.18 mW $cm^{-2}$ and the current density is 250 mA $m^{-2}$ at a stack temperature of 1272 K. The waste heat recovered from the HRSG is 558 kW with an exit gas temperature and a pressure of 453 K and 1.42 bar, respectively.

The net electrical power output (ac) of the plant is 1700.3 kW, in which 437.8 kW comes from the power turbine. The latter contributes about 25.8% to the total electrical power output. The electrical and overall (system) efficiencies of the plant are 60.6 and 80.5%, respectively. The system efficiency is defined as the ratio of the useful energy output to the lower heating value (LHV) of the fuel; the former includes the electrical energy produced by the SOFC stack and PT (in terms of ac power output), and the heat recovery at the HRSG. Excluding the heat recovery in the calculation of useful energy output, the efficiency so obtained is defined as the electrical efficiency.

The operating data of the air compressor, GT and PT are summarised in Tables 3–5, respectively. From their corrected mass flow rate, shaft speed and inlet gas parameters, it is obvious that the system components operate at full-load condition.

Under part-load operating conditions, the fuel and air flow rate to the SOFC stack are reduced in order to follow the load

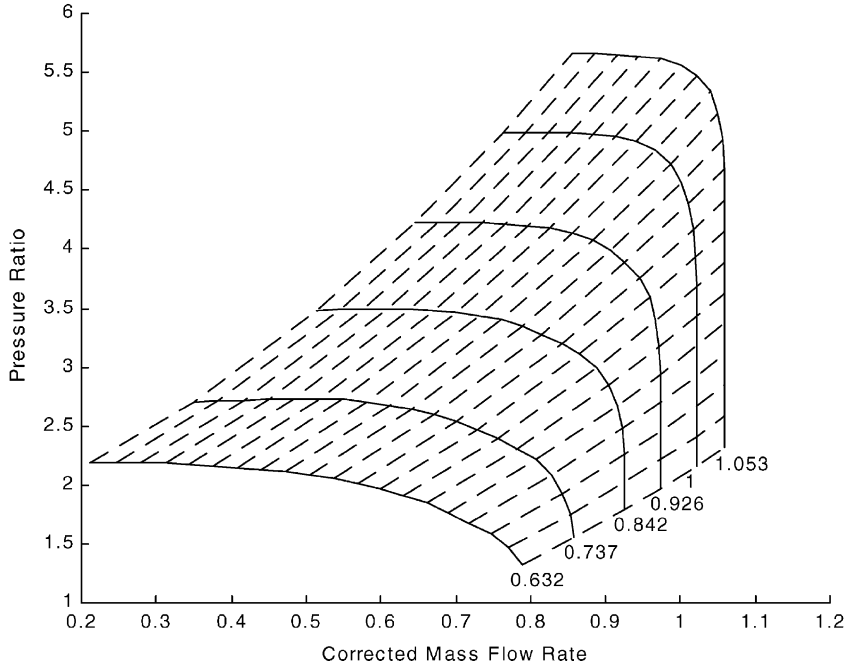


Fig. 6. Program-generated compressor map.

changes. Additional fuel flow and diluting air to the combustor are necessary, as mentioned earlier. The amount of fuel and air are assumed initially and adjusted in the simulation to meet the requirements of component matching and to achieve system thermal and mass balance. From Fig. 13, it can be seen that during part-load operations, when the load is reduced from 100 to 56.8%, the fuel flow rate through the SOFC stack is decreased from 13 to 4 kmol $h^{-1}$. The additional fuel to the combustor is increased, however, from 0 to 8.03 kmol $h^{-1}$ to maintain the normal operating status of the GT. There is only a slight change in the total fuel flow rate of the system during part-load operations. The decrease of fuel flow rate to the stack is the main cause of the reduced power output of the

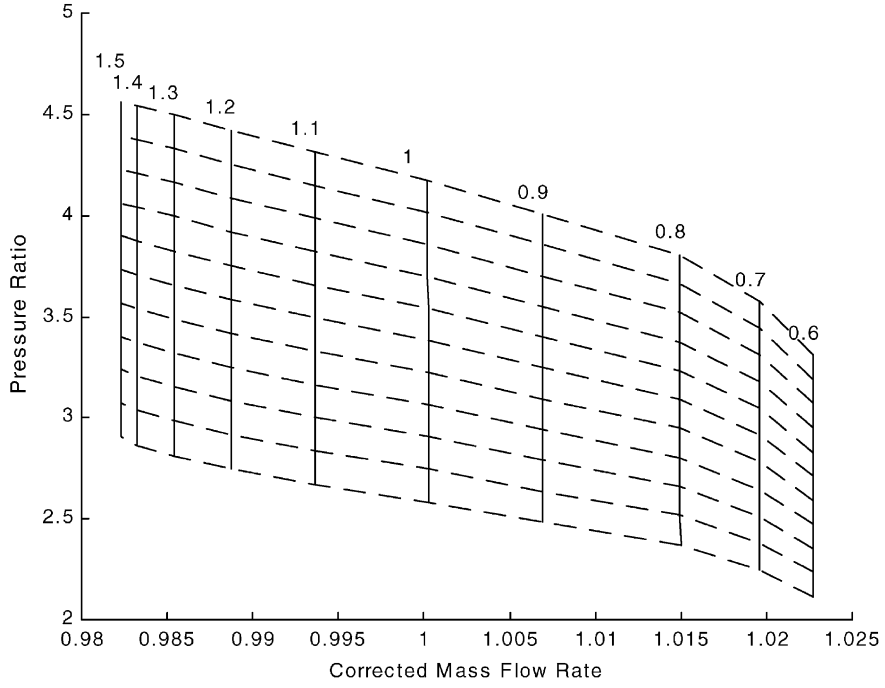


Fig. 7. Program-generated gas turbine map.

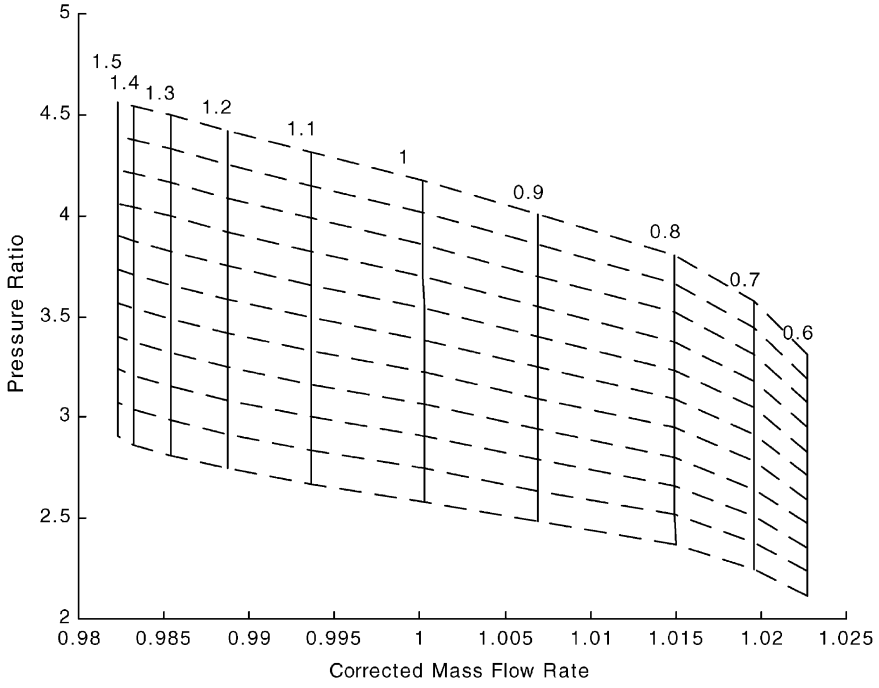


Fig. 8. Program-generated power turbine map.

system as the main source of power output is from the SOFC stack. The change of air flow rate during part-load operations is shown in Fig. 14. The air flow rate to the SOFC stack is decreased from 145 to 45 kmol $h^{-1}$, while the fuel flow rate is decreased from 13 to 4 kmol $h^{-1}$ to match the fuel cell operation. Diluting air to the combustor is increased from 100 to 190 kmol $h^{-1}$ to adjust the inlet temperature and mass flow rate of the GT. The total air flow rate varies in the range 230–245 kmol $h^{-1}$ during part-load operations.

The change of stack operating temperature and TIT when the system is switching from full-load to part-load operations is given in Fig. 15. The operating temperature of the SOC stack varies from 1272 to 1142 K, while the

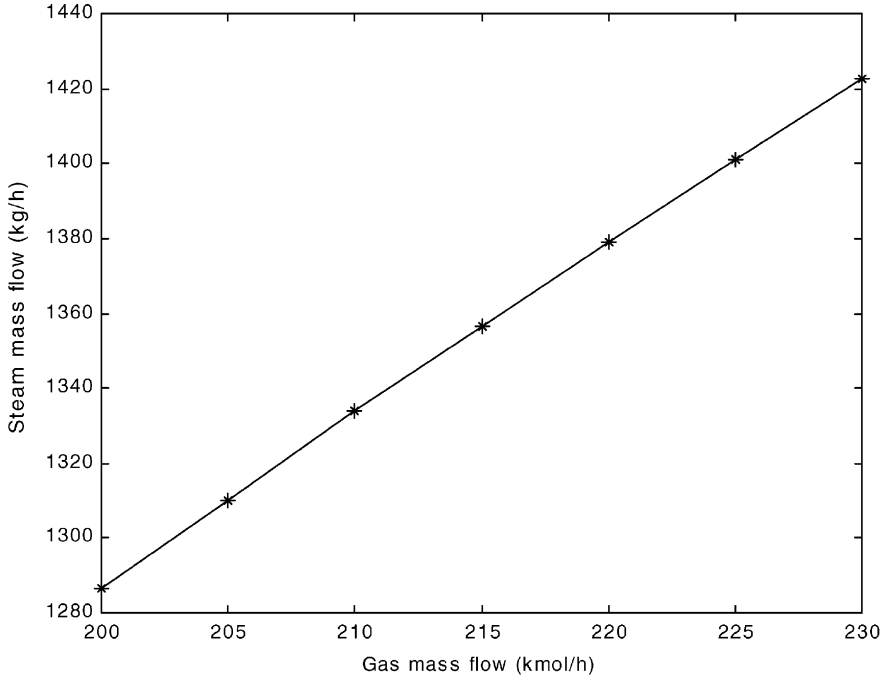


Fig. 9. Effect of gas molar flow rate on steam yield.

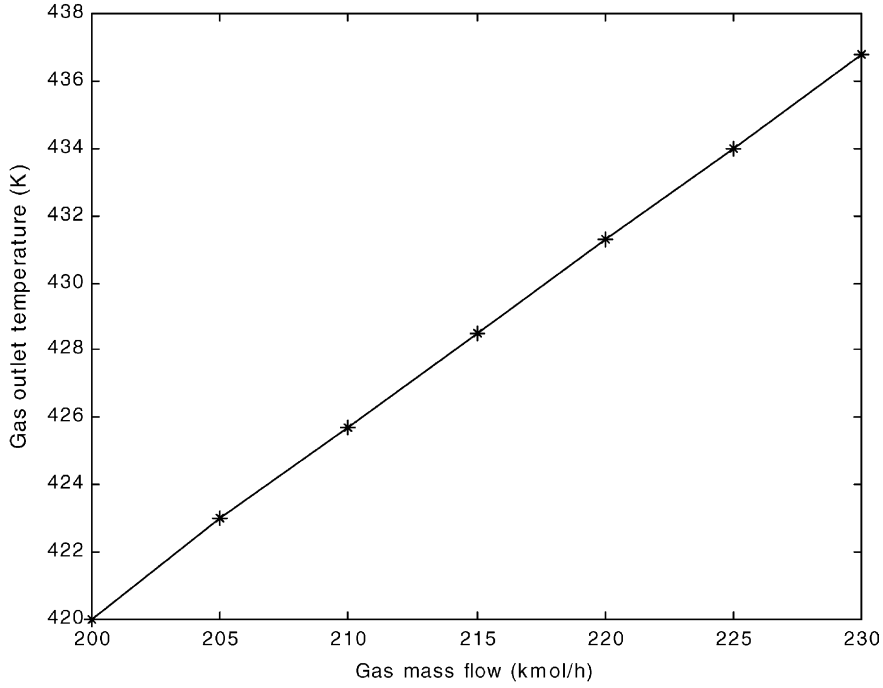


Fig. 10. Effect of gas molar flow rate on exit gas temperature of HRSG.

TIT changes between 1285 and 1367 K. These temperature ranges are suitable for SOFC and gas turbine operations.

The results shown in Fig. 16 demonstrate that the power turbine operates at its design point (∼435 kW) and is maintained at more-or-less the same power output under part-load operations, while the SOFC stack reduces its power output from 1277 to 540.6 kW when the load decreases. The decrease in stack power is due mainly to the reduced fuel flow rate and hence the reduced current density of the cell. Thus, the stack operates more efficiently at higher cell voltage [6]. The power turbine maintains a high efficiency because it operates at/near its design point. Note that, a direct comparison of the contribution in total

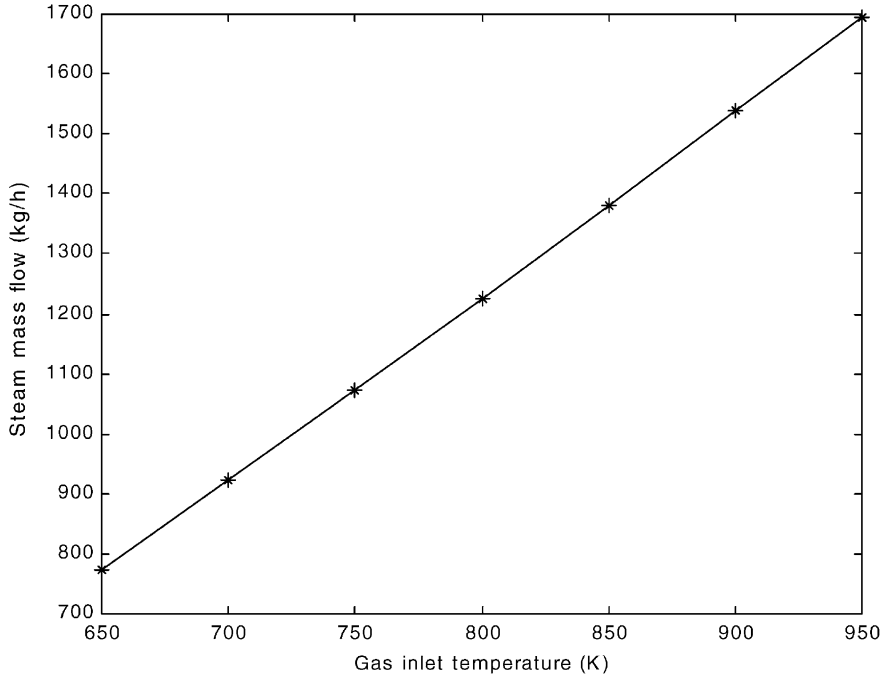


Fig. 11. Effect of gas inlet temperature on steam yield.

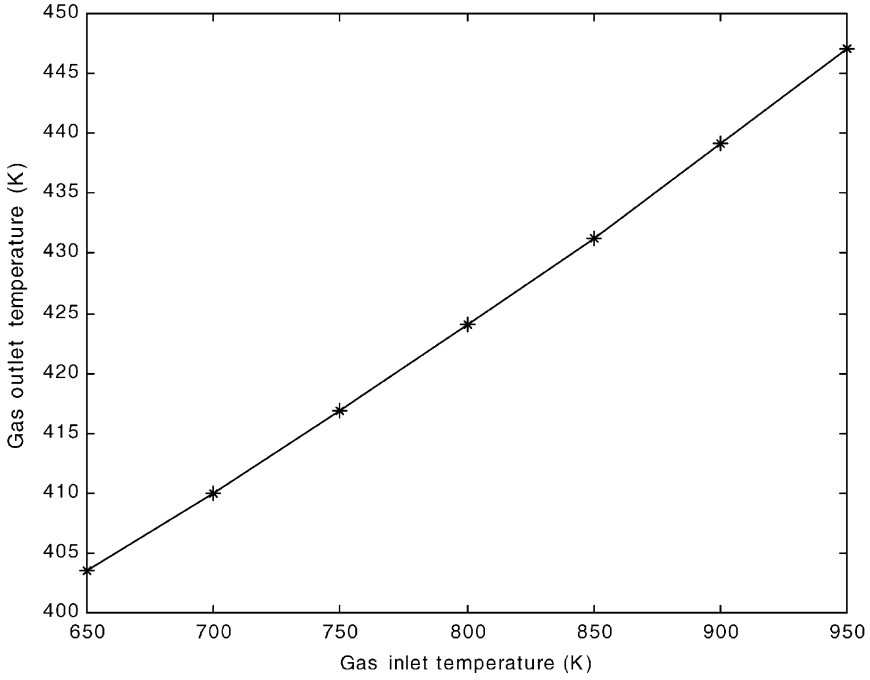


Fig. 12. Effect of gas inlet temperature on gas exit temperature of HRSG.

Table 1
System full-load operating parameters

| | |
|---|---|
| Air pressure ratio | 5 |
| Fuel pressure ratio | 4 |
| Stack air flow rate (kmol $h^{-1}$) | 145 |
| Cooling air flow rate (kmol $h^{-1}$) | 100 |
| Fuel (NG) flow rate (to SOFC stack) (kmol $h^{-1}$) | 13 |
| Total fuel (NG) flow rate (kmol $h^{-1}$) | 13 |
| Fuel utilisation | 0.85 |
| Fuel cell number | 40,000 |
| Steam/methane ratio | 2 |

Table 2
System full-load performance

| | |
|---|---|
| Cell voltage (V) | 0.619 |
| Cell current density (A $cm^{-2}$) | 250.7 |
| SOFC stack ac power output (kW) | 1276.9 |
| SOFC stack working temperature (K) | 1272 |
| Circle exit gas temperature (K) | 453 |
| Circle exit gas pressure (bar) | 1.52 |
| Air compressor work demand (kW) | 333.6 |
| Fuel compressor work demand (kW) | 14.4 |
| GT/PT gas flow rate (kg $s^{-1}$) | 2.1 |
| PT net ac output (kW) | 437.8 |
| HRSG steam generated (kg $h^{-1}$) | 479 |
| Heat recovery (kW) | 936.5 |
| Electrical efficiency (LHV) (%) | 60.6 |
| Total efficiency (LHV) (%) | 80.5 |

Table 3
Operating data of air compressor

| | |
|---|---|
| Air compressor inlet pressure (bar) | 1 |
| Air compressor inlet temperature (K) | 298 |
| Air compressor shaft speed (%) | 100 |
| Air compressor corrected mass flow (%) | 106.5 |
| Air compressor corrected speed (%) | 104.7 |
| Air compressor pressure ratio | 5 |
| Air compressor efficiency | 0.803 |

Table 4
Operating data of gas turbine

| | |
|---|---|
| GT inlet pressure (bar) | 4.6 |
| GT inlet temperature (K) | 1309 |
| GT shaft speed (same as air compressor) (%) | 100 |
| GT corrected mass flow (%) | 98.7 |
| GT corrected speed (%) | 99.7 |
| GT pressure ratio | 3.7 |
| GT efficiency | 0.926 |

Table 5
Operating data of power turbine

| | |
|---|---|
| PT inlet pressure (bar) | 3.04 |
| PT inlet temperature (K) | 1190.5 |
| PT corrected mass flow (%) | 97 |
| PT corrected speed (%) | 110 |
| PT pressure ratio | 2 |
| PT efficiency | 0.91 |

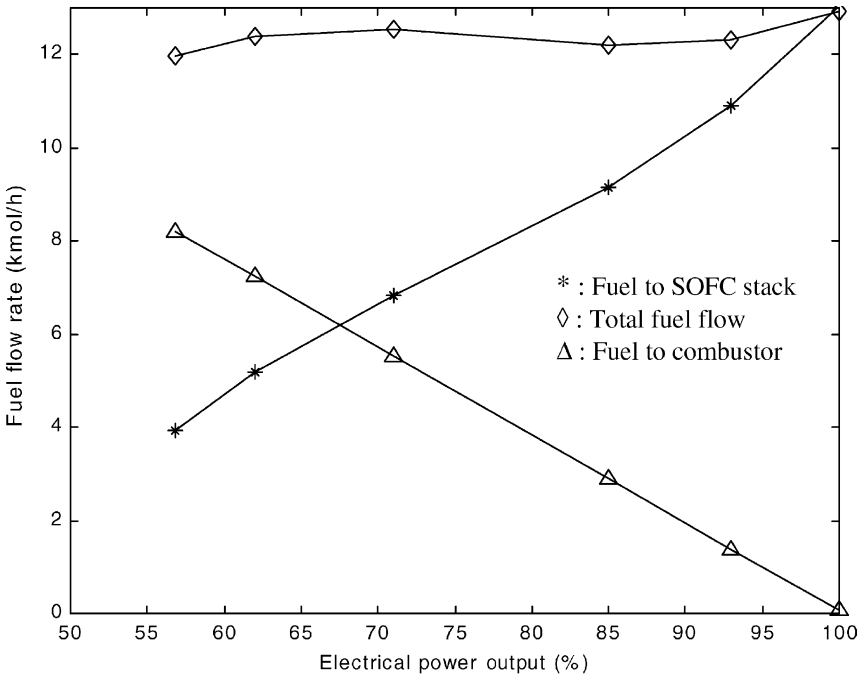


Fig. 13. Variation of fuel molar flow rates under part-load operations.

plant LHV efficiency between the GT and the fuel cell stack is not so meaningful in the case of part-load operations, because the stack uses only part of the fuel as the input while turbine makes use of the waste energy from the stack and additional fuel as the source of energy. Thus, if their respective contributions are calculated simply by judging the power output, the efficiency of the turbine may be overestimated while the stack efficiency may be underestimated.

The electrical efficiency, the amount of heat recovery and the total efficiency of the power plant are shown in Fig. 17. The electrical efficiency decreases from 60.6 to 37.4% when the power output decreases from full load to 56.8% load. This is because more fuel is directly used in the combustion

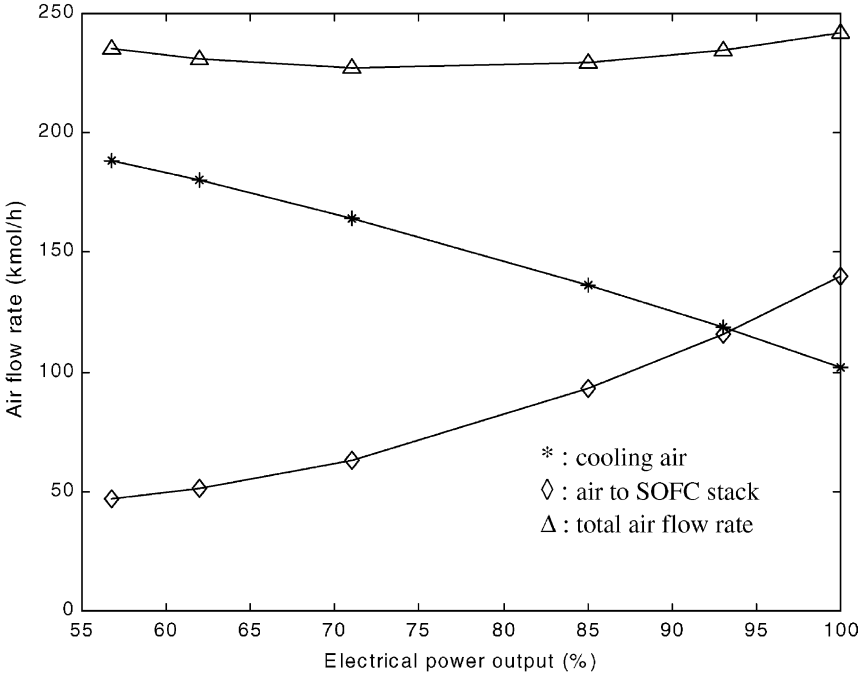


Fig. 14. Variation of air molar flow rate under part-load operations.

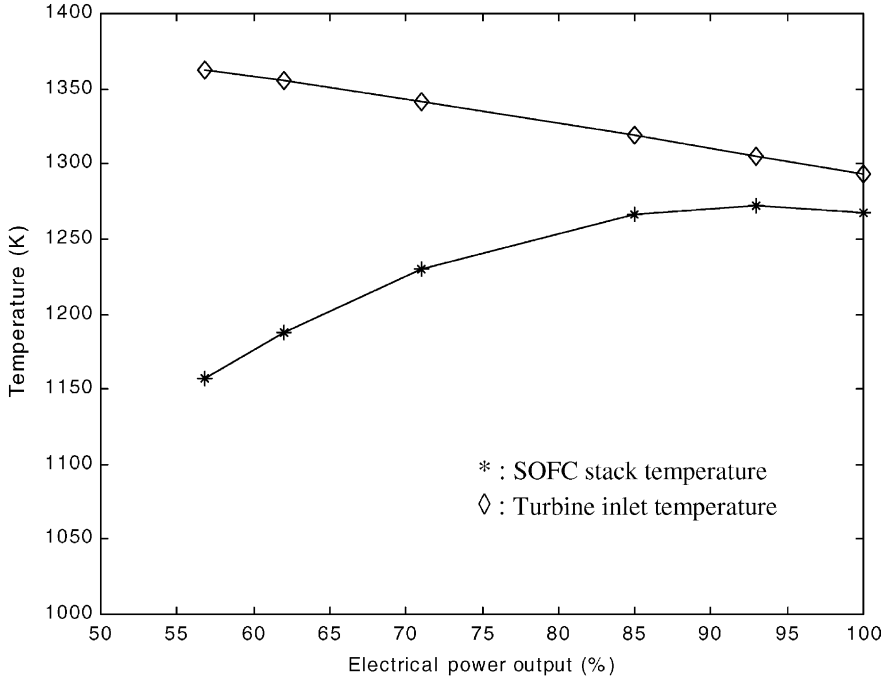


Fig. 15. Variation of SOFC stack operation temperature and turbine inlet gas temperature under part-load operations.

to improve the turbine inlet gas flow and temperature. The heat recovery increases from 19.9 to 26.8%, and this reduces the total efficiency of the plant from 80.5 to 64.2%.

Results show that the electrical efficiency is only 37.4% when the system operates at 56.8% of full load. In a sole SOFC plant, the electrical efficiency can be still very high when the system operates at part-load conditions because its efficiency is a function of cell voltage and fuel utilisation. In a SOFC–GT power system, however, the gas turbine system consumes most of the fuel by direct combustion. Thus, the total electrical efficiency is offset by the relatively poor efficiency of the turbine (compared with SOFC). In other

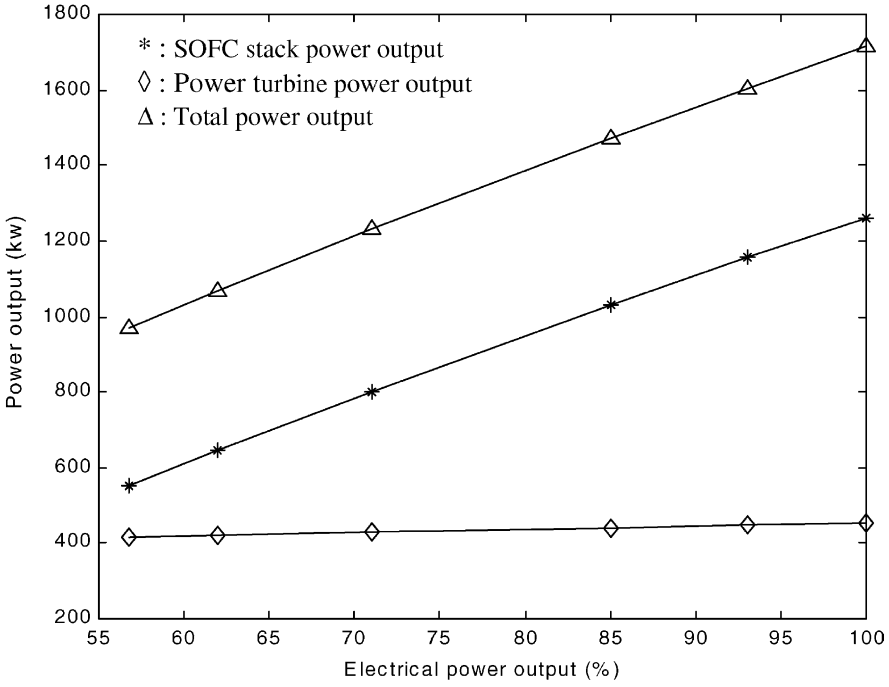


Fig. 16. Variation of SOFC stack and power turbine power output under part-load operations.

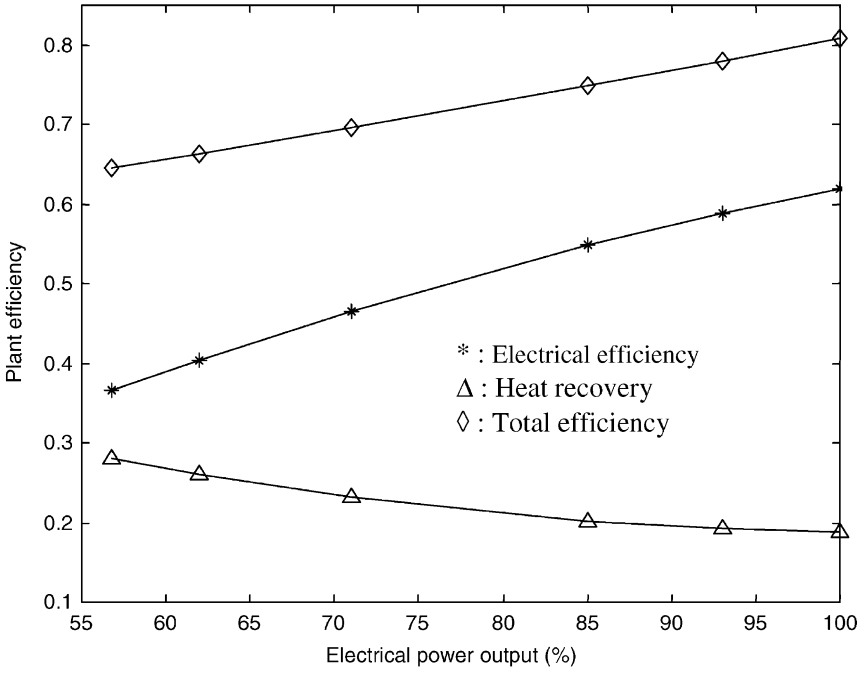


Fig. 17. Variation of plant electrical, heat recovery and total efficiency under part-load operations.

words, it is cost-effective to adopt simpler and safer operations by direct combustion of fuel to improve the gas turbine performance during part-load operations.

## 5. Conclusions

From this study, the following conclusions are drawn.

(i) Based on a typical SOFC–GT hybrid power system configuration, a code has been developed to predict the performance of the plant under full-load and part-load operating conditions. The code can simulate a wide range of power output from stationary plants by minor adjustment of the specifications of the system components. Since the system is highly thermal coupled, different levels of iterative approach have been used in the modularised program.

(ii) A strategy has been proposed for system start-up and part-load and full-load operational control. In particular, the part-load operation incorporates the inherent characteristics of a SOFC–GT hybrid system by adjusting the system power output through bypassing part of the fuel to a combustor. This enhances the upstream condition of the gas turbine and hence improves turbine performance. Though the total efficiency of the system is reduced, the operation is simpler and safe.

(iii) A discussion is presented on different strategies for small and large excursions from the designed point (full load in our case), and whether the reduced load is a short-term or long-term. The issue is basically a trade-off exercise between the efficiency and performance, and between the power and the heat (for steam generation) demands of the SOFC–GT hybrid power system.

## References

[1] W. Winkler, H. Lorenz, J. Power Sources 105 (2002) 222–227.
[2] G.J.K. Acres, J. Power Sources 100 (2001) 60–66.
[3] W. Winkler, H. Lorenz, J. Power Sources 106 (2002) 338–343.
[4] S. Campanari, Full load and part load performance prediction for integrated SOFC and microturbine systems, International Gas Turbine and Aeroengine (1999-DT-65), The American Society of Mechanical Engineers.
[5] P. Costamagna, L. Magistri, A.F. Massardo, J. Power Sources 96 (2001) 352–368.
[6] S.H. Chan, H.K. Ho, Y. Tian, J. Power Sources 109 (2002) 111–120.
[7] S.H. Chan, H.K. Ho, Y. Tian, Int. J. Hydrogen Energy, in press.
[8] H.D. Jonathan, Transient modeling and simulation of a solid oxide fuel cell (thermal, mass flow, electrochemical), Ph.D. Thesis, 1997.
[9] N.F. Bessette II, W.J. Wepfer, Chem. Eng. Commun. 147 (1996) 1–15.
[10] A.P. Fraas, Heat Exchanger Design, second ed., Wiley, New York, 1989.